УДК 533.528+621.74+539.2

Synergy Nanostructuring Carbon Materials Based on Cavitation Technologies

Liudmila V. Kashkina,
Vladimir A. Kulagin*, Olesya P. Stebeleva,
Dmitry S. Likhachev and Eleonora A. Petrakovskaya
Siberian Federal University,
79 Svobodny, Krasnoyarsk, 660041 Russia [1]

The purpose of the present paper is to obtain new physical properties and to expand a range of operational properties of various carbon-blacks by using hydrodynamic and thermophysic effects of cavitation. After the cavitation experiment the wood carbon-black has in part gained some properties of nanocomposites among which there are fullereniferous and diamond-bearing carbon-blacks. In this case cavitationally processed wood carbon-blacks can be as an efficient modifying additive in lubricants, etc

Keywords: cavitation nanotechnology, wood carbon-black, activated carbonaceos materials, nanocomposites, modifying additives, lubricants.

Introduction

Nanotechnology principles in tribology were realized in the middle of the past century in the manufacturing of engine oils additives. New opportunities have arisen from obtaining a new carbon allotropic form–fullerenes. The first foreign publications, and also patents of Japan and the USA granted in the early 90-s, have proven the fullerenes to be promising as antifrictional coatings, solid lubricants and lubricating oils additives [1].

Fullerene is a hollow spherical molecule reminding a football and consisting of sixty and more atoms of carbon. The molecule surface consists of alternating hexagons and pentagons which nodes have carbon atoms. The molecule diameter is 0.7 nanometers.

Molecules are retained in a crystal by Van der Waals forces considerably determining the macroscopic properties of solid C_{60}. The fullerene molecules are strong oxidizers because they have high electro negativity and are capable to bond to themselves up to six unbound electrons. Upon bonding to themselves the radicals of various chemical nature, the fullerenes are capable to form a wide class of chemical compounds having various physical and chemical properties [2].

Besides the fullerenes there still are nanotubes – hollow cylindrical formations from hexagons having as a rule an end spherical cover including pentagons [3]. The nanotubes result from extended graphite fragments. The tube diameter is 10-30 Á, and their length is about

---

*   Corresponding author E-mail address: v.a.kulagin@mail.ru
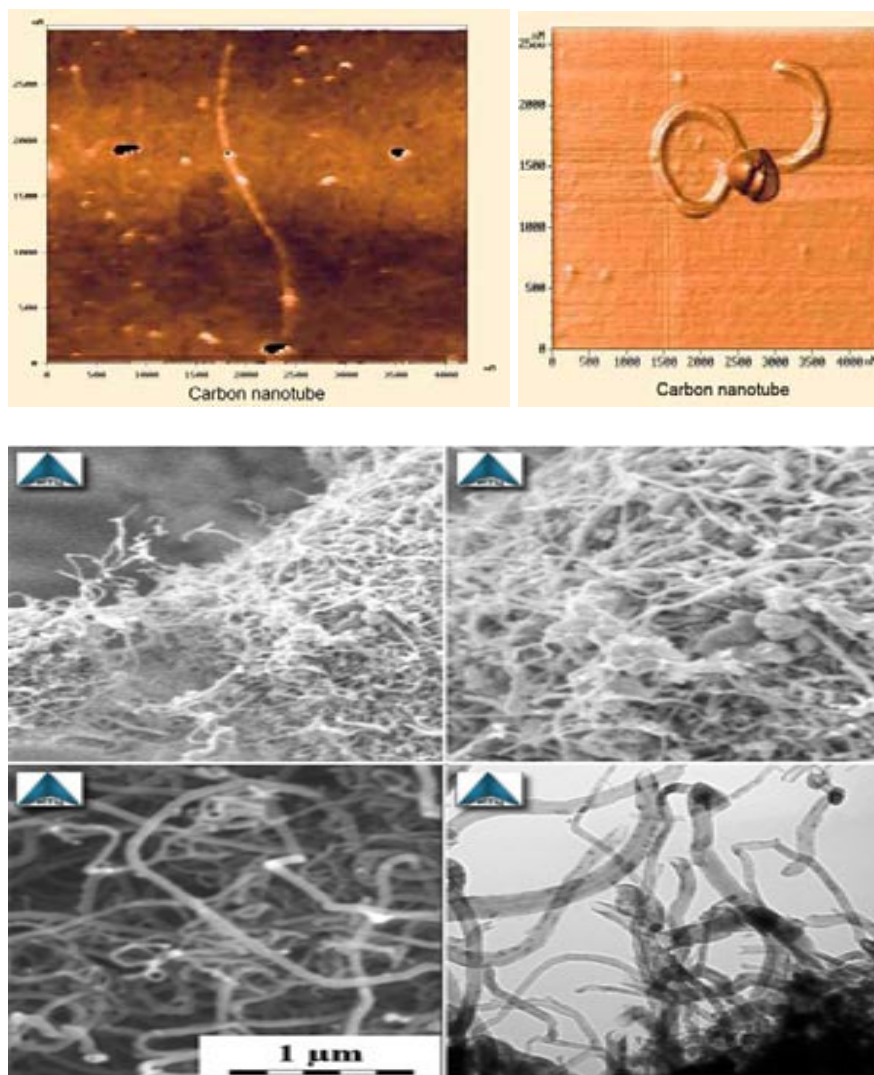[1]   © Siberian Federal University. All rights reserved

Fig. 1. Carbon nanotubes

hundreds of angstroms. The tubes can be multilayer. Vertexes of real tubes are as a rule far from ideal hemispheres.

The multilayer nanotubes can be "Russian doll" type and is a collection of single-layered nanotubes coaxially embedded into each other. Another variety is coaxial prisms coaxially embedded into each other. A third variety is a roll-type structure [3]. Embodiment of a particular nanotube structure is determined by its synthesis conditions. The presence of defects in a nanotube result in corrugating its layers. If some pentagons and heptagons are implanted into a tube surface, then this makes the tube protuberant and concave bends respectively. The tubes become bent and spiral, Fig. 1.

Fullereniferous carbon-black is obtained by pulverizing the carbon anode in arc plasma in the atmosphere of inert gas (Hafman-Krechmer method). The pulverization products settle on chilled walls of the chamber and primarily on the cathode surface. The fullerene percentage in the carbon-black is approximately up to 10-12 %.
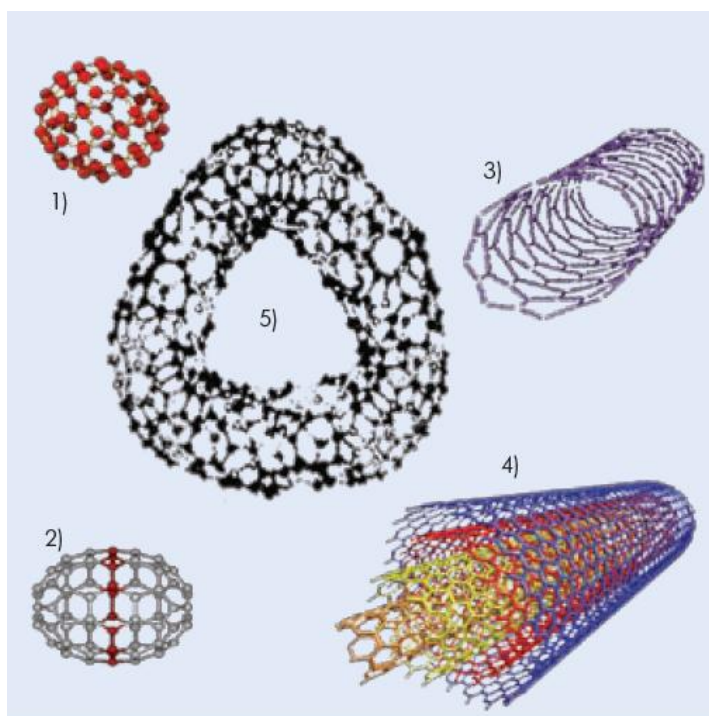
Fig. 2. The structure of most widely known fulleriods: 1 – C_{60} fullerene, 2 – C_{70} fullerene, 3 – single-shell nano-tube, 4 – multi-shell nanotube, 5 – multilayer polyhedral nanoparticle – astralene

The fullerenes in fullereniferous carbon-black can be both as fullerite and in disordered state. The investigations of the fullerenes and fullereniferous carbon-black by the method of small-angle and wide-angle X-ray patterns point to the presence of both the C_{60} crystallites of size ~20-25 nanometers and graphite crystallites of size 2-3 nanometers in an amorphous matrix. Besides the C_{60} crystallites conglomerates, there are also present conglomerates of C_{60} two molecules (dimers) [4].

The cathode precipitate is a composite agglomerate which central friable part has up to 10 % of nanotube mass, but which more consistent crust has mostly fully-variable polyhedral carbon multilayer nanostructures of fulleroid type which are called astralenes [5]. Fig. 2 gives the view of astralenes.

The multistage process of formation of fullerenes and fullereniferous carbon-black can be described as follows [6]. In the discharge active zone where the electric current flows, the plasma temperature is so high that there are only carbon atoms and ions in this zone. In the motion process from the discharge axis to the chamber wall the plasma temperature decreases and there initially starts transformation of C_2 molecules, chains, rings and multiple-ring systems (Fig. 3). Then there are formed fullerene and carbon-black particles.

In the following stage there occurs integrating of fullerenes and carbon compounds of small size into associates – zones with increased density of fullerenes.

The associates start to be shaped into nanoclusters as the move away from the fan-like plasma jet zone. Their aggregates and macroparticles of carbon-black are further generated. Probably, the formation of black wood is similar to the process of formation of fullerene-containing soot. Formation of soot globules up to 200 nm, which are then combined into associates, Fig. 4.
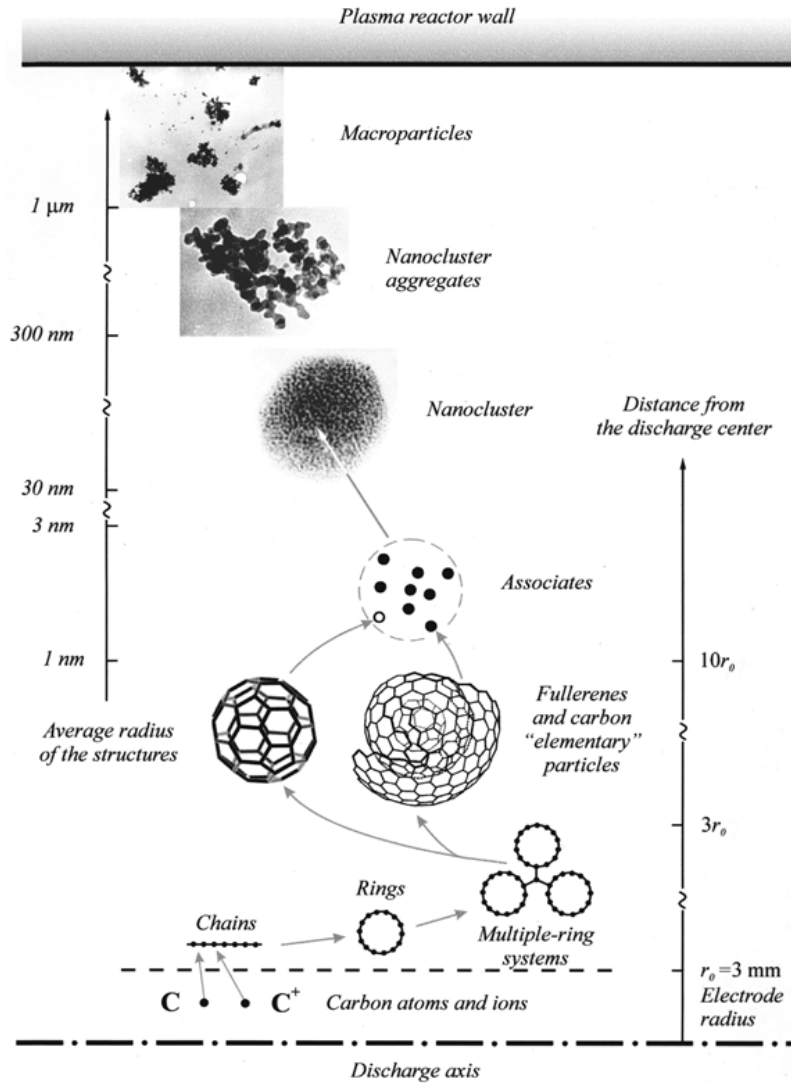
Fig. 3. Diagram of fullereniferous carbon-black formation

In B. M. Ginzburg's et al. works, there was investigated some effect of small additives of C_{60} fullerene and fullereniferous carbon-black on tribological properties of various lubricants. In doing so, it was shown that considerably lower-cost fullerene carbon- black takes practically the same effect as pure fullerene. So [7] displayed decreasing wear of steel and copper surface friction in the presence of fullerenes in the lubricant. The value of the parameter describing the surface optimization lessens, in case of copper, and gets near the reference standard value describing a minimal wear. In units with dry friction of steel on steel, the expediency of employing fullerenes as additives to lubrications is recognized by the [8] authors only in case of low pressures.

A number of works [9, 11] is devoted to the effect of fullerene carbon-black additives in polymers. And the presence of fullerene additives imparts nanocomposite properties to the samples under study. In [11] they studied the effect of fullerenes on fluoroplastics wear out of pressure and found 30 %
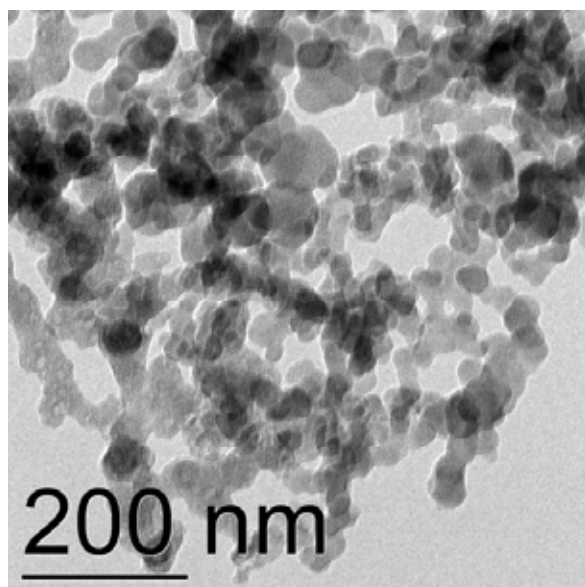
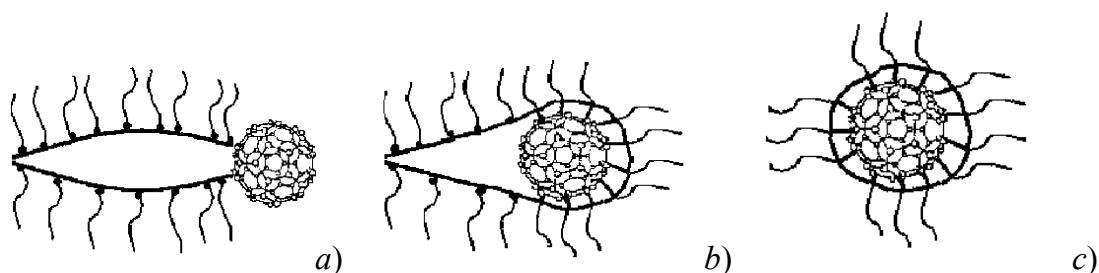Fig. 4. The original wood soot. Electron microscope JEOL JEM-X 2100.Uvelichenie x30000

a)   *b)*   *c)*

Fig. 5. Diagram of the crack extension across a polymer matrix modified with C_{60} molecules. *a* – initial stage, *b* – covalent bonds formation and partial retraction of a C_{60} molecule into the microcrack, *c* – complete retraction of the C_{60} molecule into the microcrack

increase of load-bearing at introducing 1 % of fullereniferous carbon-black. Thus it is shown that considerably lower-cost fullerene carbon-black takes practically the same effect as pure fullerene. There has been made the following conclusion: the role of fullerene comes to the initiation of processes of tribopolymerization of hydrocarbons which are in mineral oils and the formation of a protective polymer film on friction surface.

In work [11] they suggested a hypothetical mechanism of hardening effect of fullerene carbon-black at friction. The electron shells of fulleroids are characterized by the presence of a great quantity of delocalized π-*conjugate* electrons. A mechanical destruction of polymer chains is effected under mechanical destruction of the polymers in the mouth of generated microcracks. Apparently an analogous process takes place in the mouths of numerous microcracks resulting in wear particles formation. Fig. 5 gives a diagram of the crack extension reaching the C_{60} molecule (or small conglomerate). Free polymeric radicals concentrate on the microcrack surface (Fig. 5 *a*). Some of them having reached the fullerene surface, forms with fullerene. On further increasing the

forces that open the crack, these bonds split and there occurs retracting a C_{60} molecule (or aggregate of molecules) into the microcrack (Fig. 5 *b*), going with generation of a greater number of new covalent bonds of polymeric radicals with fullerene that finally results in «healing» the microcrack (Fig. 5 *c*).

There has been made the following conclusion: the role of fullerene comes to the initiation of processes of tribopolymerization of naphthene and paraffin oligomers which are in mineral oils and the formation of a protective polymer film on friction surface (a molecular bearing).

In the recent years there are made attempts of creating so-called friction geomodifiers – additives created on the basis of natural materials or nanoparticles, or both, which take effect both on tribological properties of a lubricant and on the structure and properties of the solid surfaces participating in friction In [12] there are effects of using new dry-lubricant mixture including silicate minerals of layer structure and surface-active nanoparticles present in initial carbon-black obtained in an electric arc of electrolysis electrodes. It has made for reducing the friction coefficient and increasing wear resistance of friction units, cutting power costs and improving vibronoise features of support structures of mechanisms and machines. It is known that some minerals of layer structure (such as mica, kaoline clay, graphite, etc.) are widely used as thickening and wear-proof additives [13]. Their positive effect is caused by ability of these minerals to form thin films on friction surfaces consisting of flake particles oriented parallel to fiction surface.

At introducing ultradisperse powders of diamond-graphite into greases, the friction coefficient decreases by 14-40 % and in some cases up to 60 % depending on the basic grease. Properties and the role of such powders in a grease are still under studying [10].

The purpose of the present paper is to obtain new physical properties and to expand a range of operational properties of various carbon-blacks by using hydrodynamic and thermophysic effects of cavitation. The technique of hydrodynamic effect is given in detail in [14-16].

Research methodologies

Conducted short-term treatment of cavitation water suspensions with a concentration of blacks from 10^{-3} to 10^{-2} wt. %. Experiments were performed with cuneiform cavitator (the vertex angle of the wedge was 60º) at room temperature. The magnitude of rotor revolutions varied from 5000 up to 20000 rpm. Processing time was up to 2 min.

After the experiment, slurry was poured into a Petri dish and defended at room temperature until complete evaporation of water. Dried sediments were studied. In the process of cavitation, an increase in temperature of the water suspension (at 10-50 °C) depending on the speed and time of rotation of the rotor.

The principal problem in the cavitation motion pattern is determining the impact pressure in fluid at the moment of the vapor bubble collapse. The Rayleigh equation and its solution for collapsing spherical cavity in perfect liquid is as follows:

$$T = \frac{1}{3}\sqrt{\frac{3}{2}\frac{\rho_1}{\Delta p}}\, a_0 B\left(\frac{5}{6}, \frac{1}{2}\right),$$
(1)

where T – is the time of collapsing the spherical cavity, ρ_1 is fluid density, Δp – is non-equilibrium pressure differential, a_0 – is the initial radius of sphere, $B(x, y)$ – is beta function.

After the collapse of a bubbler the kinetic energy also becomes equal to null, however, under the energy conservation law it does not disappear completely but is conversed to elastic energy of some fluid macrovolume as a result of a hydraulic impact. Calculations show, e.g., that for a bubbler with an initial radius $a = 1$ mm in collapsing there is a hydraulic impact $p = 3.12 \cdot 10^8$ Pa $= 3120$ atm.

The non-equilibrium structure that has emerged as a result of a hydraulic impact, generates a shock wave which front pressure diminishes under the law:

$$P_{уд}\left(r\right) = P_{\max}\frac{a_*^2}{r^2}.$$

where α_* – is the initial radius of a bubble.

Already within 10 α_* distances from the centre of a collapsed bubble the pressure at the front sharply drops down to 3 atm and becomes safe from the point of view of cavitation erosion. Thus the bubbles collapsed near the cavitating surface, have the greatest destroying effect. At the first stage of bubble collapse all other forces – viscous friction, surface-tension and pressure – are less powerful than inertial forces and are continuously increasing due to magnification of velocity and the decreasing of the bubble radius. At the second stage the viscous friction force which is proportional to interphase boundary velocity, starts increasing as well as the surface tension force does to a lesser degree. Perhaps because of energy dissipation, there occurs the heating of fluid surface layer that causes intensive water evaporation in a bubble and hydraulic impact lessening at the last stage of the bubble collapse. The vicinity around the bubble after «collapse» can be considered as plasma. Indeed, when the collapses in a local volume, then there are formed fields of high pressure (up to 2000 MPa) near and inside it. The interphase boundary velocity at the cavitation microbubble collapse can attain 500 m/s and depends on its radius. The collapse of the bubble adiabatically occurs within submicroseconds and the temperature therewith rises up to 10^3-10^4 K.

The mechanism of cavitation processing effect is caused by spatial pictures of relief-compression waves as a result of cavitation bubbles collapse. As this takes place, there emerge rapidly changing fields of high pressures and temperatures and also some turbulent microstreams causing the medium micromixing [14, 15].

In the manufacture of composite materials the cavitation effect (the erosive destruction mechanism and intensive turbulent micromixing) makes for obtaining high-dispersion substrata and mixtures.

Studying the performance of carbon systems including various carbon-blacks under the external effects such as cavitation, electrohydraulic discharge, etc., is rather urgent on account of their wide industrial application.

The experiment has been performed on the following types of carbon-blacks:

• fulleniferous carbon-black obtained by a plasma-arc process of graphite rods evaporation in discharged helium atmosphere (manufactured by the Open Joint-Stock Corporation «New Tech Product», St. Petersburg). Two samples have been studied. The C_{60} fullerene content was wt. 11 % and wt. 0.1 %;

• diamond-bearing carbon-black;

• wood carbon-black.

Cavitation processing was carried out on carbon-black water suspensions (5 mg of carbon-black per 100 ml of water; 58.5 mg of carbon-black per 100 ml of water). The rotor rotation

speed in the cavitation mixer was from 5000 up to 20000 rpm, the time of processing was 1-2 minutes. In the cavitation process there was water suspension temperature rise (by 10-50°C) depending on speed and time of the rotor rotation. The time of suspensions sedimentation was long enough.

Interpretation and discussion of research results

After the experiment a part of the suspension was poured out into a Petri dish and settled until complete evaporation of water at room temperature. The samples elemental source composition was determined by the Bruker X-ray fluorescent spectrometer S-4 Pioneer which accuracy is not worse than 0.001 % depending on the element. The samples composition of fullereniferous carbon-black is presented in the Table 1.

The major portion of fullereniferous carbon-black samples is carbon (99.92 %). Nevertheless, there are also small amounts of paramagnetic impurities (nickel, iron, zinc, copper, cobalt). Composition of samples of wood soot are shown in Table 2, which shows that the sample of 94.58 % consists of carbon, and the remaining 5 % are impurities.

The X-ray phase analysis spectra have shown (Figs. 6-8) that in the initial carbon-blacks there is a considerable amount of impurities (iron oxides, copper oxides, various aluminum silicates). The shape of the X-ray phase analysis spectrum changes after the cavitation effect (Fig. 9)

The wide shape of a spectrum indicates that there has occurred additional dispersion in the sample in spite of the fact that it already had nanostructures as diamond nanoparticles.

Table 1

	The fullerene concentration 0.1 wt. %	The fullerene concentration 11 wt. %		The fullerene concentration 0.1 wt. %	The fullerene concentration 11 wt. %
C	99.92	99.92	Ca		0.0033
Na	0.0059	0.0071	Cr	0.0012	
Mg	0.0024	0.0016	Fe	0.0033	0.0028
Al	0.0012	0.0041	Co	0.0006	
Si	0.018	0.019	Ni	0.002	0.0018
P	0.003	0.0015	Cu	0.0036	0.0039
S	0.015	0.013	Zn	0.003	0.0028
Cl	0.018	0.022			

Table 2

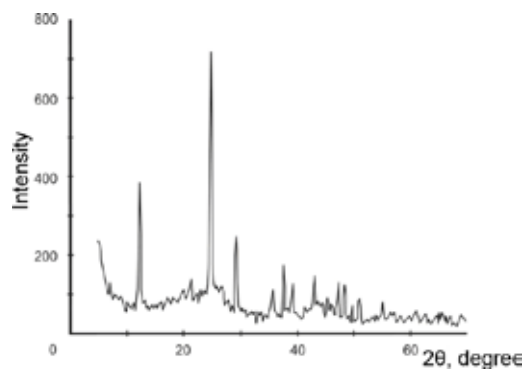|	Wood carbon-black, wt. %		Wood carbon-black, wt. %
C	94.58	Cr	0.356
Na	0.1	Fe	0.11
Mg	0.18	Co	0.373
Al	0.382	Ni	0.639
Ca	0.1	Cu	3.001
		Zn	0.0759

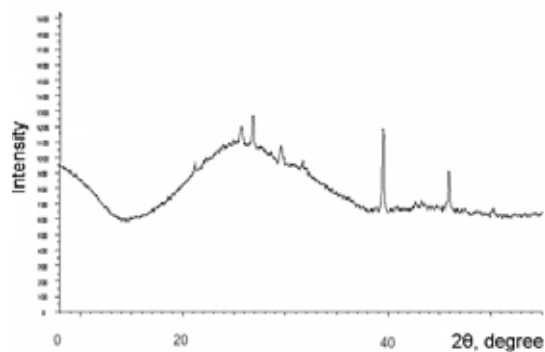Fig. 6. X-ray phase analysis spectrum of diamond-bearing carbon-black

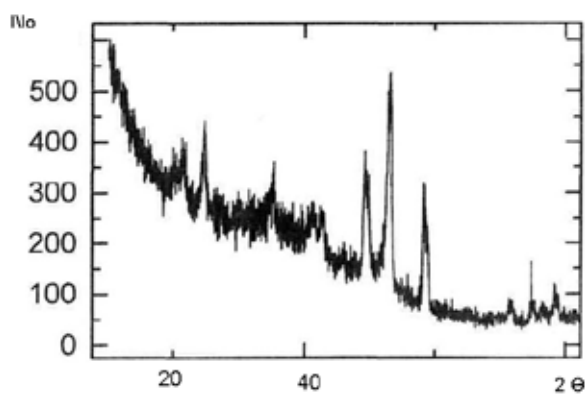Fig. 7. X-ray phase analysis spectrum of wood carbon-black

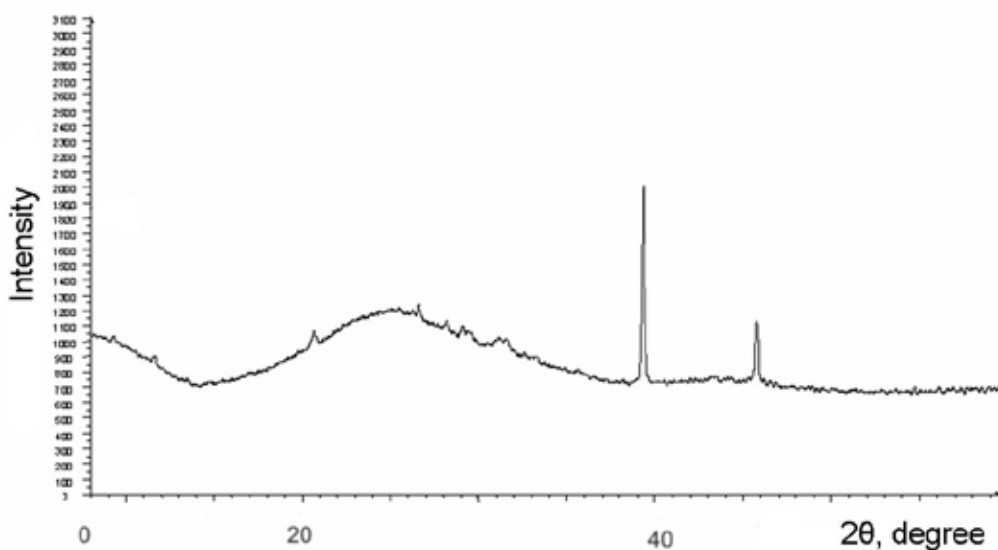Fig. 8. X-ray phase analysis spectrum of fullereniferous carbon-black with 11 wt. % fullerene content

Fig. 9. X-ray phase analysis spectrum of diamond-bearing carbon-black after cavitation

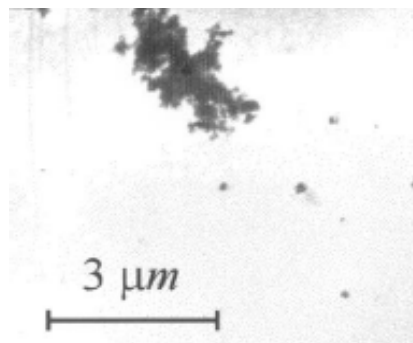Fig. 10. A carbon-black particle. 1400^X microscope magnification

Fig. 11. A fullereniferous carbon-black particle

Characteristic optical images of sediments for all types of investigated carbon-blacks are presented in Figs. 10-13. The shape of a sediment is compared to that of the nanotubes described in the literature [3].

At low magnification fullerene soot is qualitatively similar to conventional carbon black (Figs.10-11).
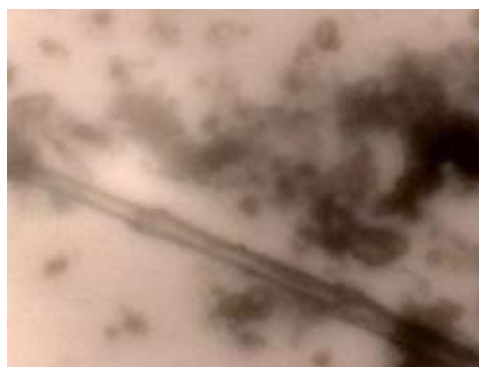
Sediments of all carbon-blacks after cavitation, in addition show evidence of generated macroparticles and molecular aggregates in the shape of various straight and bent tubular structures intertwined and bent bundles (Figs. 11-14). There are also aggregates in the shape of chains which thickness uniformly changes their full length. The molecular aggregates that are observable in the experiment and the nanotubes described in the literature, are similar in their shape but differ by 3-4 orders lengthwise, by 2 orders in diameter. The bending angle of molecular formations is 180° as it is seen in the presented Figures. This property is inherent in the nanotubes which are not only considerably durable but also flexible.
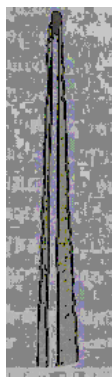
Nanotubes images
(reference data)

Optical macroimages of the carbon-black
sediment after cavitation

a)

b)

Fig. 12. a) Mace-like nanotubes with a periodic movement of the wall thickness; b) Tubular molecule aggregates. 100^X microscope magnification

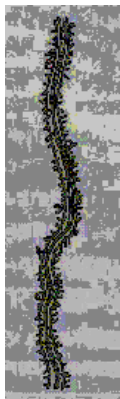Nanotubes images
(reference data)

Optical macroimages of the carbon-black
sediment after cavitation

a)

b)

Fig. 13. *a*) Nanotubes covered with a layer of amorphous carbon (reference data); *b*) Tubular molecule aggregates. 100^X microscope magnification

Nanotubes images
(reference data)

Optical macroimages of the carbon-black
sediment after cavitation

a)

b)

Fig. 14. a) Nanotubes covered with graphite flakes; b) Tubular molecule aggregates. 100^X microscope magnification

a)

b)

Fig. 15. Tubular molecule aggregates in fullereniferous carbon-black (11 wt. % C$_{60}$) after cavitation 15000 rpm. Microscope magnification *a*) 2800^X, *b*) 1400^X

Molecular aggregation of carbon-black particles after cavitation in the shape near to that of nanotubes, is seen in the sediments of all carbon-blacks. At the same time and under the same parameters of the cavitation experiment (cavitator rotation speed, duration of rotation), the chain molecular aggregates in the sediments of wood carbon-black are detected in smaller quantities than in the sediments of fulleriferous and diamond-bearing carbon-blacks (Fig. 15).

The electronic paramagnetic resonance (EPR) was carried out on the EPR spectrometer SE/X-2544. The resonance was observed on a frequency of $v = 9$ GHz (wave length $\lambda = 3$ cm). The spectrum shape of the EPR fulleriferous carbon-black (11 wt. % C_{60}) is given in Fig. 16.

The EPR spectra shape changed after the cavitation processing. Fig. 17 gives a spectrum of the EPR fulleriferous carbon-black (11 wt. % C_{60}) after processing in the cavitation mixer at the angular speed of rotor rotation 20000 rpm. during 50 sec.

At 293 K the spectrum of EPR consists of a central narrow line and a wide line. The wide line is caused by the presence of iron oxide and as it is supported by the fact that at 77 K we can see this line diminish its intensity and its broadening occurs. It can be connected with the presence of superparamagnetic particles in the sample. As a result of the cavitation effect, large paramagnetic particles of iron implement superparamagnetic transition. It is indicative of not only changing the shape of the EPR line but also of reducing the *g-factor* from 3 up to 2.26.

Fig. 18 illustrates a spectrum of the EPR of the same sample after simple rotation in a mixer (without a cavitator) at an angular speed of rotation 20000 rpm. The EPR spectra presented in Figs. 17 and 18 are of different shape which is indicative of an important change of fulleriferous carbon-black structure under the cavitation effect.

The analysis of the EPR of the spectrum of initial diamond-bearing carbon-black presented in Fig. 19 has shown that at cooling a sample down to the temperature of liquid nitrogen (77 K) the line of a radical broadens which is typical for nanostructural formations, among them, diamond nanoparticles. After the cavitation effect the line of the radical vanishes (Fig. 20). The vanishment of the line of the radical in the EPR spectrum can follow the initial structure destruction and shaping a new structure.
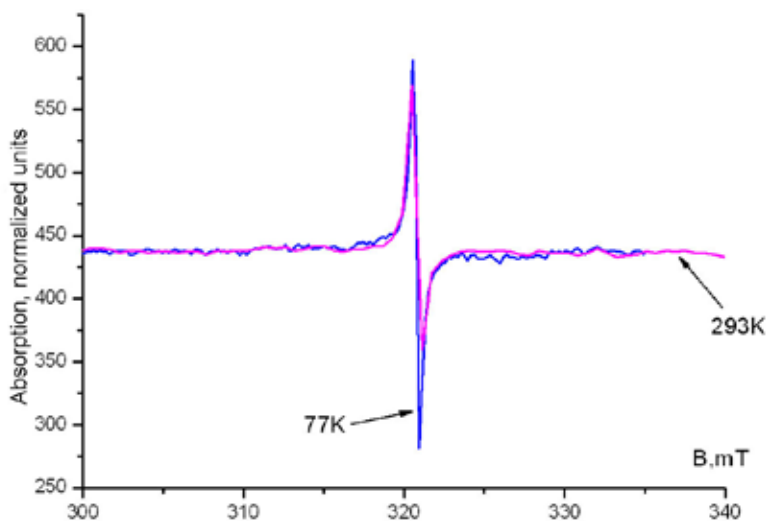

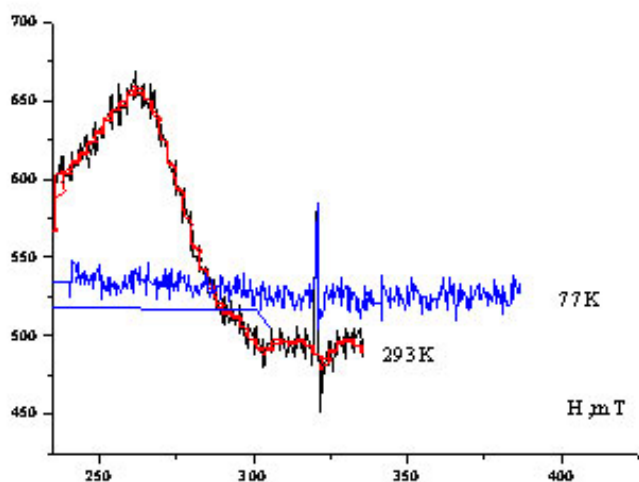Fig. 16. Spectrum of the EPR initial carbon-black with 11 % C_{60} content

Fig. 17. Spectrum of the EPR carbon-black (11 wt. % C_{60}). Rotor rotation speed 20000 rpm. Mixing with the cavitator
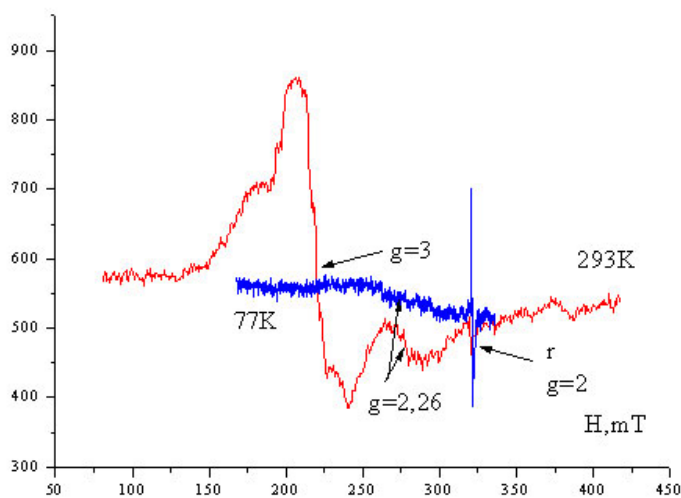

Fig. 18. Spectrum of the EPR carbon-black (11 wt. % C_{60}). Rotor rotation speed 20000 rpm. Mixing without the cavitator

This assumption is supported by the X-ray phase analysis and optical microscopy data above, i.e. after cavitation there has occurred additional dispesion of powder already containing nanostructures.

Fig. 21 and 22 shows the EPR spectra of wood soot. The shape of the EPR spectra at kavitatsiolnnoy treatment varies similarly diamond soot. There is a broadening of the line, changing the *g-factor*.

Summary and Conclusions

As mentioned above, the cavitation experiment was carried out with two types of carbon-blacks: those that showed themselves very well in solving tribological problems (fulfereniferous and diamond-bearing)
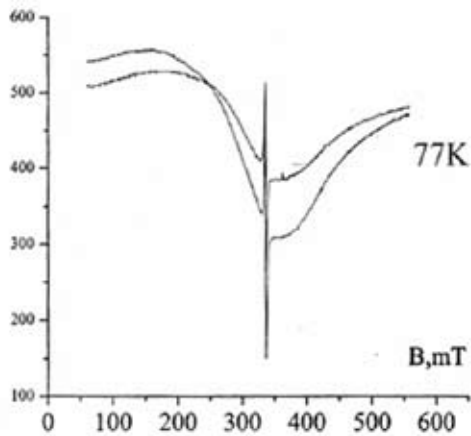
Fig. 19. The EPR spectrum of diamond-bearing carbon-black

Fig. 20. The EPR spectrum of diamond-bearing carbon-black after cavitation processing
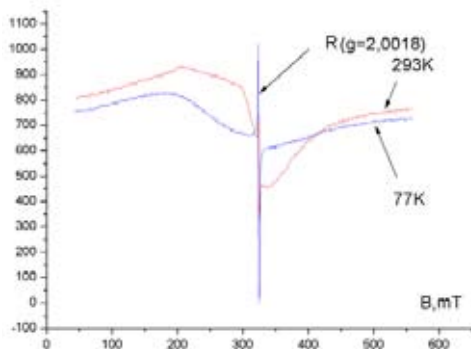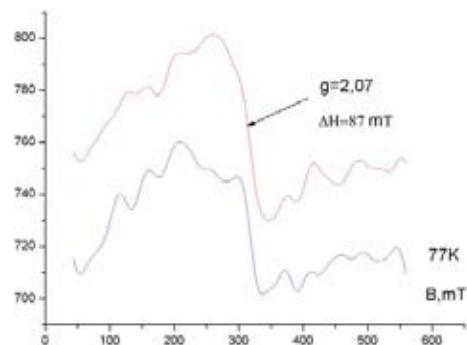

Fig. 21. The EPR spectrum of wood carbon-black

Fig. 22. The EPR spectrum of wood carbon-black after cavitation processing

[1,7-10,13] and the carbon-black that was not studied yet (wood carbon-black). As a result of the there have been obtained suspensions of all the carbon-blacks with long sedimentation time that points to their significant dispersion [16]. A molecular aggregation of carbon-black particles which is identical in the shape to nanotubes was observed in the dried sediments of all the carbon-blacks.

There is intense cavitation effect on the electronic structure of the samples. Time of sedimentation of suspensions treated with soot dramatically increased. So for cavitation-treated fullerene soot sedimentation time was about 6 months, for wood soot – more than 2 months. These values are much higher since the initial sedimentation of carbon black suspensions.

It may be concluded that after the cavitation experiment the wood carbon-black has in part gained some properties of nanocomposites among which there are fullereniferous and diamond-bearing carbon-blacks. Hence, an opportunity has appeared to use it for solving various tribological problems instead of expensive fullereniferous and diamond-bearing carbon-blacks. In this case cavitationally processed wood carbon-blacks can be as an efficient modifying additive in lubricants, etc.

References

1. Ginzburg, B. M. Research and development of new types of antifriction and antiwear materials on the fullerene base / B. M. Ginzburg, D. G. Tochilnikov // Problems of engineering industry and reliability of machinery. 2002. – № 2.

2. Fullerenes: Synthesis and formation theory / G. N. Churilov, N. V. Bulina, A. S. Fedorov; ed. V. F. Shabanov. – Novosibirsk: Publishing House of the Siberian Branch of the Russian Academy of Science, 2007. – 230 p.

3. Rakov, E. G. Nanotubes and fullerenes. – M: Logos, 2006.

4. Ponomarev, A. N. Polyhedral multilayer carbon nanostructures of fulleroid type / A.N. Ponomarev, V. A. Nikitin // The Russian Federation Patent; № 2196731. Date of the publication: 20.01.2003.

5. Gorelik, O. P. Cluster structure of fulfereniferous carbon-black particles and C60 fullerene powder / O. P. Gorelik, G. A. Dyuzhev, D. V. Novikov, et al. // The Journal of Theoretical Physics. 2000. – V. 70. – № 11. – P. 118-125.

6. Ginzburg, B. M. Research of structure of powdered C60 fullerene and fullerene carbon-black by the method of small-angle X-ray radiography / B. M. Ginzburg, Sh. Tuychiev, S. Kh. Tabarov, A. A. Shepelevsky // Crystallography. 2007. – V. 52. – № 2. – P. 211-214.

7. Ginzburg, B. M. Effect of C60 fullerene carbon-blacks and other carbon materials on boundary friction of metals sliding / B. M. Ginzburg, O. F. Kireyenko, M. V. Baydakova, et al. // The Journal of Theoretical Physics. 2000. – V. 70. – № 12. – P. 87-97.

8. Ginzburg, B. M. Effect of coupling agent and C60 fullerene on solid lubricating coating properties / B. M. Ginzburg, D. G. Tochilnikov // The Journal of Theoretical Physics. 2000. – V. 70. – № 1. – P. 94-99.

9. Ginzburg, B. M. Tribological property of composite materials of polytetrafluoroethylene-fullerene carbon-black / B. M. Ginzburg, A. O. Pozdnyakov, D. G. Tochilnikov, et al. // High-molecular compounds. 2008. – V. 50. – № 8. – P. 1483-1492.

10. Operating capacity of sliding bearing assemblies in boundary lubrication requirements / V. F. Terentyev, N. V. Erkaev, S. I. Tschelkanov; ed. I. O. Bogulsky. – Novosibirsk: Nauka, 2006. – 219 p.

11. Ginzburg, B. M. On mechanisms of wear strength magnification of composites on the base of polytetrafluoroethylene doped with fullerene carbon-black / B. M. Ginzburg, D. G. Tochilnikov, A. A. Shepelevsky, et al. // Letters to the Journal of Theoretical Physics. 2007. – V. 33. – № 20. – P. 88-94.

12. Yakhyev, N. Ya. Lubricating composition for improving tribologic features of a lubricant / N. Ya. Yakhyev, Zh. B. Begov, Sh. D. Batyrmurzaev, et al. // Friction, wear, lubricant. www.tribo.ru, 2008. – V. 10. – № 3.

13. Wolkov, V. P. Application of finely dispersed natural hydrosilicates and nanoparticles to modify rubbing surfaces / V. P. Volkov, K. A. Pavlov, N. N. Loznetsova // Friction and lubrication in machines and mechanisms, 2006. – № 12. – P. 3-5.

14. Ivchenko, V. M. Cavitation technology / V. M. Ivchenko, V. A. Kulagin, A. F. Nemchin; ed. G. V. Logvinovich. – Krasnoyarsk: KGU Publishing House, 1990. – 200 p.

15. Kulagin, V. A. Nanotechnology cavitational effects in the heat-and-power engineering and other branches of production / V. A. Kulagin, L. V. Kulagina, T. A. Kulagina // Journal of Siberian Federal University. Engineering & Technologies 1 (2008) 76 – 85.

16. Kashkina, L. V. Study the Effects of Cavitation Dispersion of Doping Solid Materials / L. V. Kashkina, V. A. Kulagin, O. P. Stebeleva, L. V. Kulagina // Energy in a Globalized World: Sat. thesis, coincides with reports of the First International Science and Technology Congress. – Krasnoyarsk: ООО Verso, 2010. P. 415-417.

Вопросы синергизма наноструктурирования углеродных материалов на основе кавитационной технологии

Л.В. Кашкина,
В.А. Кулагин, О.П. Стебелева,
Д.С. Лихачев, Э.А. Петраковская
Сибирский федеральный университет,
Россия 660041, Красноярск, пр. Свободный,79

Цель данной работы – получить новый уровень физических свойств и расширить диапазон эксплуатационных свойств различных саж, используя гидродинамические и теплофизические эффекты кавитации. Древесная сажа после кавитационной обработки частично приобретает свойства нанокомпозитов, к которым относятся фуллерено- и алмазосодержащие сажи. В этом случае кавитационно-обработанные древесные сажи могут выступать в качестве эффективной модифицирующей добавки в смазочные материалы и т.д., взамен дорогостоящих фуллерено- и алмазосодержащих саж.

Ключевые слова: кавитационная нанотехнология, древесная сажа, активированные углеродосодержащие материалы, нанокомпозиты, модифицирующие добавки, смазочные материалы.